




# Exploring and attributing change to fractional vegetation coverage in the middle and lower reaches of Hanjiang River Basin, China

Yi Yan · Huan Liu · Xixuan Bai  ·  
Wenhao Zhang · Sen Wang · Jiahuan Luo ·  
Yanmin Cao

Received: 18 March 2022 / Accepted: 19 October 2022 / Published online: 21 November 2022  
© The Author(s), under exclusive licence to Springer Nature Switzerland AG 2022

**Abstract** The middle and lower reaches of Hanjiang River Basin (MLHB), areas that have an important ecological function in China, have experienced great changes in the vegetation ecosystem driven by natural environmental change and human activity. Here, we explored the spatio-temporal dynamics of fractional vegetation coverage (FVC) and quantitatively analyzed its driving factors to advance current understanding of how the ecological environment has changed. Specifically, we used the dimidiate pixel model to calculate the FVC of the MLHB from 2001 to 2018 based on Moderate Resolution Imaging Spectroradiometer (MODIS) Enhanced Vegetation Index (EVI) data. We then used Theil–Sen median slope (Sen’s slope) and coefficient of variation (CV) to explore spatial and temporal variations, as well as characteristics in fluctuations. Finally, we

utilized a geographical detector model (with spatial scale effects and spatial data discretization tests) to quantify the influence of the detected natural and human factors. Results showed that average annual FVC was 0.30–0.75 for ~90% of the study area over the 19-year study period with a heterogeneous spatial distribution. FVC variation trend displayed stability and improvement. Areas with higher FVC displayed greater stability. All 10 detected natural and anthropogenic factors were responsible for changes in FVC. The primary factors causing FVC to change were precipitation (in 2001) and slope (in 2018), followed by landform type, distance to water, and nighttime light (NTL) (in 2018). Precipitation and slope consistently displayed the largest interaction across all years. The interaction between human and topographical factors had gradually increasing significance on changes in FVC over the research period. The range and type of factors suitable for promoting vegetation growth were detected in the study area. Results of this study can provide a scientific basis for developing effective strategies for local vegetation protection, restoration, and land resource management.

**Supplementary Information** The online version contains supplementary material available at <https://doi.org/10.1007/s10661-022-10681-w>.

Y. Yan · H. Liu · W. Zhang · S. Wang · J. Luo · Y. Cao  
Key Laboratory of Resources Conversion and Pollution  
Control of the State Ethnic Affairs Commission,  
College of Resources and Environmental Science,  
South-Central Minzu University, Wuhan 430074,  
People’s Republic of China

X. Bai (✉)  
School of Civil Engineering and Architecture, Wuhan  
Institute of Technology, Wuhan 430074, China  
e-mail: baixx87@wit.edu.cn

**Keywords** Vegetation · Attribution analysis ·  
Natural factors · Human activity · Hanjiang River  
Basin

## Introduction

Vegetation is an important component of the terrestrial ecosystem and plays a significant role in climate change, carbon cycle, water retention, and soil erosion prevention (De Boer, 1983; Kong et al., 2018; Sun et al., 2015; Walther et al., 2002; Zuazo & Pleguezuelo, 2008). As such, vegetation is regarded as an integrated indicator for monitoring changes to the ecological environment (Wang et al., 2015). Under the influence of both natural and human activities, the process of vegetation change exhibits complex characteristics (Piao et al., 2003). Consequently, a hot topic in academic research involves developing ways to obtain a detailed understanding of this process, including analyses of response mechanisms of changes to vegetation in relation to natural and human activity at regional and global scales (Feng et al., 2020; Xu et al., 2020b; Zhao et al., 2018). Therefore, mapping time series of vegetation change and comprehending the change mechanism are essential for global and regional ecological environmental protection and restoration.

Fractional vegetation coverage (FVC) defined as the ratio of the vertical projected area of green vegetation (including leaves, stems, and branches) on the ground (Shoshany et al., 1996; Wu et al., 2019) is an important index for describing vegetation growth and for reflecting ecosystem changes (Iizuka et al., 2019; Purevdorj et al., 1998). It is widely used to monitor ground vegetation coverage at different scales (Li et al., 2004; Wang et al., 2016a). Detecting trends in changes to FVC, and associated spatial variation, provides information on the dynamic of vegetation coverage, allowing areas subject to degradation or requiring restoration to be identified. In this regard, FVC is a good indicator for reflecting vegetation condition.

Remote sensing technology provides dynamic real-time information, allowing wide coverage and repeatable observations (Verbesselt et al., 2012; Volpe et al., 2011). As such, it provides technical support for monitoring and evaluation of vegetation coverage and has become the main technology used in vegetation coverage research (Yang et al., 2013). Remotely sensed vegetation indices based on the dimidiate pixel model (DPM) are most widely used to estimate FVC (Yan et al., 2022). This method is widely and successfully applied for extracting vegetation cover at multiple scales for its simplicity and high accuracy (Ding et al., 2016; Wu et al., 2014; Yan et al.,

2022). Therefore, the FVC estimated by remote sensing images and DPM has become a feasible method of vegetation ecosystem monitoring.

Vegetation coverage is sensitive to changes in the natural environment and human activity, reflecting the impact over a certain period (Jiang et al., 2021; Tang et al., 2021; Zhang et al., 2021). The mechanisms by which vegetation changes are influenced in complex ways by both natural and human factors vary across regions (Li et al., 2021; Peng et al., 2019; Yang et al., 2021; Zhang et al., 2022). It is a great challenge to identify the underlying driving factors to vegetation coverage change and quantify their influence. Most existing studies have primarily evaluated how natural factors impact FVC, rather than human factors. Furthermore, existing research tended to adopt multivariate statistical analysis to identify relationships between vegetation coverage and potential driving factors (Feng et al., 2020; Li et al., 2017; Qu et al., 2020) without consideration of spatial heterogeneity. Moreover, traditional statistical methods require linearity and normal distribution. In contrast, the geographical detector model can detect numerical and qualitative data without needing to follow the requirements of multivariate statistical methods (Yun et al., 2019) and can be used to identify spatial differences in environmental change effectively. Thus, this approach has been widely and successfully used to assess the individual influencing factors and their interactions on vegetation change and can elucidate the mechanism of vegetation change in terrestrial ecosystems (Liu et al., 2021; Nie et al., 2021).

The Hanjiang River is an important tributary of the Yangtze River in China (Zhang et al., 2013). The Hanjiang River Basin is a typical area that is sensitive to climate change (Jin et al., 2021) and has a fragile ecological environment (He et al., 2015). The basin is also an area of key ecological function nationally, as it is a strategic area guaranteeing water resources (Deng et al., 2021; Hong et al., 2016). Consequently, protection of the ecological environment in this area is a major responsibility (Wang et al., 2018). Over the last half century, the middle and lower reaches of Hanjiang River Basin (MLHB) have been subject to drying through various factors, including regional climate warming, the construction and operation of the Danjiangkou reservoir and cascade dams, water diversion by the Middle Route Project of South to North Water Diversion (Zhuan et al., 2018), and

socio-economic development. As such, habitat conditions in this region are complex, with regional ecosystems being disturbed in ways never previously encountered. Vegetation coverage is an important indicator of change to the terrestrial ecological environment at a regional scale (Cao et al., 2014). Several studies have previously assessed change to the pattern of vegetation cover and potential driving factors in the MLHB. However, factors driving spatial and temporal changes to vegetation cover have not been comprehensively assessed, with a stronger focus on individual natural factors.

Therefore, in this study, we used the geographical detector model to quantify the factors driving changes to vegetation, and the influence of their interactions, in a humid river valley plain in China. The objectives of this study were (1) to determine temporal and spatial variations in FVC, (2) to identify the main natural and human factors driving changes to FVC, (3) to evaluate how interactions of detected driving factors alter FVC, and (4) to explore the suitable range or type of detected factors for FVC. This study is expected to advance current understanding on spatial distribution characteristics, driving factors, and interactions of changes to FVC and to identify areas at risk. Results of this work might provide a reference for studies on FVC change in other humid river valley regions. It was also conducive to further research

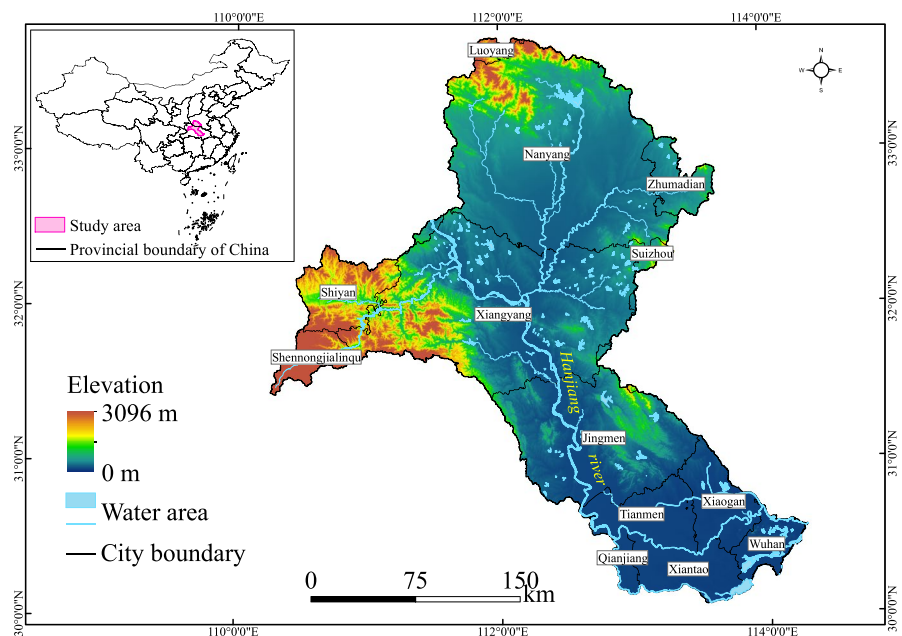
involved in predicting changing trends of FVC, allowing development of proper vegetation restoration measures. It could also be applied to quantitative evaluations on ecological environmental protection and restoration at regional scale. Understanding the spatial and temporal dynamics in characteristics of vegetation cover and potential driving forces is expected to provide beneficial baseline scientific information for protecting and restoring the regional ecological environment, as well as harmonious development of economic and social environments in the Hanjiang River Basin.

### Materials and methods

#### Study area

The MLHB encompasses the Hanjiang hydrological basin downstream of Danjiangkou Reservoir (Tian et al., 2019; Yang et al., 2020). The area covers approximately  $6.4 \times 10^4 \text{ km}^2$  (110–115° E, 30–34° N; Fig. 1). The river flows through Danjiangkou, Laohekou, Xiangyang, Yicheng, Zhongxiang, Shayang, Tianmen, Qianjiang, Xiantao, Hanchuan, and Caidian, including the counties under their jurisdiction (Rao, 2012). The MLHB belongs to the subtropical monsoon region and is subject to both drought and flooding. In general, 75%

**Fig. 1** Location of the middle and lower reaches of Hanjiang River Basin (MLHB) in China



of total annual precipitation (range: 700–1200 mm) occurs from May to September, with average annual temperatures of 15–17 °C (Wang et al., 2016c). The terrain comprises of hills and plains, of which 51.6% is plains and platform areas, 25.4% is mountainous, and 23% is hilly (Zhang et al., 2020b). This region encompasses a variety of soil types, including yellow brown, red, aquic, paddy, and purple soils (He et al., 2015). The main vegetation type of the basin is subtropical evergreen broad-leaved forest (Wang et al., 2019a). As one of the key economic development areas in Hubei Province, the ecological environment in the MLHB is of great importance (Chen et al., 2007). This region is impacted by changes to both natural environmental conditions and increasing human activity. Due to fast growth of the human population and rapid development of the local economy and urbanization, the ecological environment of the study area has noticeably changed (Zhan et al., 2021).

#### Data sources

Enhanced vegetation index (EVI), precipitation, temperature, digital elevation model (DEM), slope, landform type, soil type, vegetation type, land use type, population density (Pd), and nighttime light (NTL) data were used.

Moderate Resolution Imaging Spectroradiometer (MODIS) product MOD13Q1 EVI data (h27v05), with a temporal resolution of 16 days and a spatial resolution of 250 m, from 2001 to 2018 was acquired from the Atmosphere Archive & Distribution System Distributed Active Archive Center (LAADS DAAC) of the National Aeronautics and Space Administration (NASA) (<https://ladsweb.modaps.eosdis.nasa.gov/>). In total, 414 EVI images were used for this analysis with data of high quality that had been processed with radiation, atmospheric, and geometric corrections and widely used for studying regional vegetation previously. Images were further projected to UTM WGS 84 Zone 49 N with MODIS Reprojection Tool (MRT), to preserve spatial resolution and further extract them to the extent of the study area. The maximum value composition (MVC) method (Holben, 1986) was used to obtain monthly MODIS EVI data. Then, average of monthly data yielded annual EVI data to avoid the influence of extreme climate on vegetation growth (Qu et al., 2020).

Based on MODIS EVI data, FVC was derived using the dimidiate pixel model (Gutman & Ignatov, 1998; Mu et al., 2018), which assumes spectral information of one pixel is linearly weighted synthesized by only two components (Carlson & Ripley, 1997). The calculation formula is as follows:

$$FVC = (EVI - EVI_{soil}) / (EVI_{veg} - EVI_{soil}) \quad (1)$$

where EVI is the enhanced vegetation index of a mixed pixel, and  $EVI_{veg}$  and  $EVI_{soil}$  are values of pure vegetation and bare soil pixels, respectively (Zhang et al., 2013). Due to differences in environmental backgrounds and image quality,  $EVI_{soil}$  and  $EVI_{veg}$  changed with time and space. In the actual calculation process, the maximum and minimum EVI values of each land use type in the corresponding period were used to replace  $EVI_{soil}$  and  $EVI_{veg}$ . Based on land use types, 5% and 95% confidence levels were used to select the maximum and minimum thresholds of EVI data in the corresponding periods (Li et al., 2004).

Climate factors affect surface vegetation coverage, especially changes in precipitation and temperature (Sun et al., 2020). The meteorological data (yearly precipitation and air temperature) from 2001 to 2018 were acquired from the Chinese Meteorological Administration (<http://data.cma.cn/>). Approximately 700 meteorological stations in China were selected. Spatial distribution of precipitation and air temperature was predicted using ANUSPLIN interpolation software.

Elevation and slope were used as topographic factors to examine changes to the spatial pattern of vegetation. They were obtained using images from the NASA Shuttle Radar Topography Mission (SRTM) dataset, with a spatial resolution of 90 m, and downloaded from the Geospatial Data Cloud (<http://www.gscloud.cn/>).

Landform, soil, and vegetation type in the study area were extracted from 1:1,000,000 thematic maps delivered by the Data Center of Chinese Academy of Resources and Environmental Sciences (<http://www.resdc.cn/>).

Human influence was determined from distribution of population density and nighttime lighting. Population density data were downloaded from WorldPop (<https://www.worldpop.org/project/categories?id=18>) with 1 km resolution. Nighttime light data were downloaded from Harvard Dataverse (<https://dataverse>).

harvard.edu/dataset.xhtml?persistentId=doi:10.7910/DVN/YGIVCD) at 500 m resolution. Land use type data (including water body distribution) were acquired from the Chinese Academy of Resources and Environmental Sciences at a resolution of 30 m.

All data were reprojected to UTM 49 N WGS 84 and were resampled to 250 m to be consistent with the EVI data.

Methods

Temporal fluctuation characteristics of FVC

To detect the trends in changes to regional vegetation coverage, the Sen trend (Sen, 1968) degree of vegetation coverage from 2000 to 2018 was calculated, and the Mann–Kendall (MK) test (Fernandes & Leblanc, 2005; Kendall, 1948; Mann, 1945) was performed.

The Sen trend analysis is a method with nonparametric statistical testing and is free from data noise (Gilbert & Richard, 1987). The trend is calculated as

$$\beta = \text{median}\left(\frac{x_j - x_i}{j - i}\right) \tag{2}$$

where  $\beta$  represents the tendency of FVC,  $i$  and  $j$  represent the time series, and  $x_i$  and  $x_j$  denote FVC value at time  $i$  and  $j$ , respectively. When,  $\beta > 0$  change to vegetation coverage increases, and when,  $\beta < 0$  change declines.

The Mann–Kendall statistics were used to test the significance of the change trend (Kendall, 1948). Based on Sen’s slope and MK test results, annual mean FVC values were allocated to five classes (Table 1 in the Appendix).

Spatial fluctuation characteristics of FVC

The coefficient of variation (CV) is used to describe fluctuation degree in time series data (Xu, 2002). We applied CV to represent the stability in FVC change. The formula for CV is

$$C_v = \frac{1}{\bar{x}} \sqrt{\frac{\sum_{i=1}^n (x_i - \bar{x})^2}{n - 1}} \tag{3}$$

where  $C_v$  is the CV,  $i$  is the time series (year),  $x_i$  is FVC value at time  $i$ , and  $\bar{x}$  represents the average FVC during the study period. Obtained  $C_v$  values were further divided

into five levels: low fluctuation ( $C_v < 0.05$ ), relatively low fluctuation ( $0.05 \leq C_v \leq 0.10$ ), moderate fluctuation ( $0.10 \leq C_v \leq 0.15$ ), relatively high fluctuation ( $0.15 \leq C_v \leq 0.20$ ), and high fluctuation ( $C_v \geq 0.20$ ).

Geographical detector model

The geographical detector model is a new statistical method used to detect spatial stratified heterogeneity (Wang et al., 2016a; Xu et al., 2020a) and to reveal the factors driving it (Wang et al., 2010). The main principle of the model is that if an independent variable has an important influence on the dependent variable, then spatial distributions of the independent variable and the dependent variable should be similar in spatial distribution (Han et al., 2021; Wang & Hu, 2012; Xu et al., 2018). The geographical detector model has four modules (Wang et al., 2010): factor, risk, interaction, and ecological detectors. We used the factor, interaction, and risk detectors to detect which factors have greater influence on FVC change, determine how different factors interact with each other, and identify where vegetation grows better.

FVC values in 2001 (first year of the study period), 2009 (midpoint year of the study period), and 2018 (final year of the study period) were chosen respectively as the dependent variable in the model analysis to represent the change process. Through a comprehensive consideration of possible influencing factors on vegetation coverage in the study area and data availability, 10 factors covering climate, topography, geomorphology, soil, vegetation, water, and human activity were selected as independent variables for further model analysis (Table 1).

**Factor detector** Factor detection is represented by  $q$  value (Wang et al., 2016b) as

$$q = 1 - \frac{\sum_{h=1}^L N_h \sigma_h^2}{N \sigma^2} = 1 - \frac{SSW}{SST} \tag{4}$$

$$SSW = \sum_{h=1}^L N_h \sigma_h^2, SST = N \sigma^2 \tag{5}$$

where  $q$  represents the explanatory power of detect factor  $x$  on spatial distribution of detected factor  $y$ .

**Table 1** Information on selected factors

Aspect	Factor	Code	Unit
Climate	Mean annual precipitation	$x_1$	mm
	Mean annual temperature	$x_2$	°C
Topography	Elevation	$x_3$	m
	Slope	$x_4$	°
Geomorphology	Landform type	$x_5$	Categorical
Soil	Soil type	$x_6$	Categorical
Vegetation	Vegetation type	$x_7$	Categorical
Water	Distance to water	$x_8$	km
Human activity	Population density (Pd)	$x_9$	People/km <sup>2</sup>
	Nighttime light (NTL)	$x_{10}$	W/km <sup>2</sup>

The value of  $q$  ranges from 0 to 1; a larger  $q$  value demonstrates a greater effect of independent variable  $x$  to dependent variable  $y$ .  $h = 1, \dots, L$  is the strata of variable  $y$  or factor  $x$ ;  $N_h$  and  $N$  are the number of cells in layer  $h$  and the entire region, respectively;  $\sigma_h^2$  and  $\sigma^2$  are the variance of  $y$  values of layer  $h$  and the whole study area, respectively; SSW and SST are within and total sum of squares, respectively.

The factor detector was used to represent the influence of 10 selected natural and human factors on FVC, and a calculated  $q$  value indicates the explanatory power of FVC.

It is important to select the appropriate spatial scale and spatial data discretization method (Wang & Xu, 2017) to analyze changes to FVC and potential driving factors when using the geographical detector model. The parameter optimization, including optimization of spatial discretization method and spatial scale (Song et al., 2020), was taken into consideration. Scale effects of  $q$  values and the ranks of 10 factors were tested using eight scales (2 km, 3 km, 5 km, 8 km, 10 km, 12 km, 15 km, and 20 km). Four common methods (manual, natural break, quantile break, equal interval break) for spatial data discretization were tested to choose the optimal for the geographical detector model.

**Interaction detector** The interaction detector is used to assess the explanatory power of independent variables  $x_1$  and  $x_2$  to dependent variable  $y$ .  $q$  values

**Table 2** Types of interaction between two variables and their interactive impact

Interaction relationship	Interaction
$q(x_1 \cap x_2) < \min(q(x_1), q(x_2))$	Weaken; nonlinear
$\min(q(x_1), q(x_2)) < q(x_1 \cap x_2) < \max(q(x_1), q(x_2))$	Weaken; univariate
$q(x_1 \cap x_2) > \max(q(x_1), q(x_2))$	Enhanced; mutually
$q(x_1 \cap x_2) = q(x_1) + q(x_2)$	Independent
$q(x_1 \cap x_2) > q(x_1) + q(x_2)$	Enhanced; nonlinearly

of  $x_1$ ,  $x_2$ , and  $x_1 \cap x_2$  are calculated, respectively. The interaction type between  $x_1$  and  $x_2$  can be identified by comparing  $q(x_1)$ ,  $q(x_2)$ , and  $q(x_1 \cap x_2)$  values. The detailed interactive relationship is represented in Table 2. The interaction detector was used to examine whether selected natural and human factors have an interactive effect on FVC change.

**Risk detector** The risk detector is used to compare a significant difference of average values between subregions, which is examined by  $t$  statistics. It is calculated as

$$t_{\bar{Y}_{h=1} - \bar{Y}_{h=2}} = \frac{\bar{Y}_{h=1} - \bar{Y}_{h=2}}{\left[ \frac{\text{Var}(\bar{Y}_{h=1})}{N_{h=1}} + \frac{\text{Var}(\bar{Y}_{h=2})}{N_{h=2}} \right]^{1/2}} \tag{6}$$

where  $\bar{Y}_h$  denotes the mean value of attributes in subregion  $h$ ,  $N_h$  is the number of sample units in subregion  $h$ , and Var represents the variance.

## Results

### Spatial and temporal patterns to change in FVC

The long-term average FVC was 0.52 for the whole study area from 2001 to 2018, and the average annual FVC was 0.30–0.75 for ~90% of the study area (Fig. 2a, b). Spatial distribution of FVC in MLHB was heterogeneous, and medium-coverage, medium-low, and medium-high-coverage zones were widely distributed and relatively concentrated (Fig. 2b, Table 2 in the Appendix). Relatively high FVC values were primarily located in the mid-southern and western

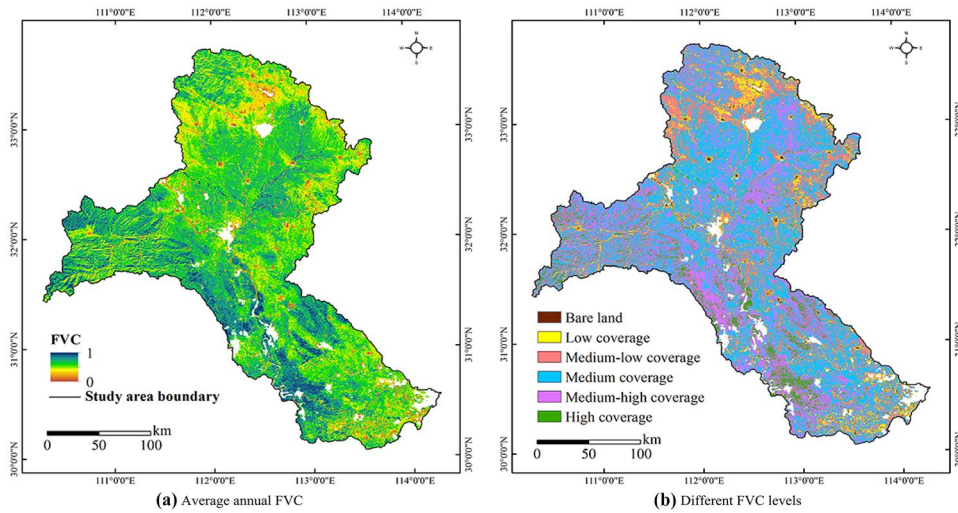


**Fig. 2** a, b Characteristics of annual mean FVC in MLHB from 2001 to 2018.

parts of the study area. Relatively low FVC values were located in the northern part of the study area and along the banks of the northernmost and southernmost sections of MLHB.

Figure 3a shows significant changes to spatial distribution in FVC from 2001 to 2018. Basically stable zones were widely distributed throughout, covering 51.99% of the study area. Areal proportion was the largest of all significance classes (Table 3). FVC declined in 23.45% of the total area, of which 18.25% showed a significant decline. These areas were mainly distributed along the banks of Hanjiang River and its tributaries in the central and southern parts of the study area. FVC increased in 24.56% of the total area, of which 19.21% showed a significant increase. These areas were relatively dispersed throughout the study area, but were mainly distributed on the northern plain.

FVC in the study area was relatively stable from 2001 to 2018 (Fig. 3b, Table 4). Areas with higher

FVC displayed greater stability. Furthermore, relatively high fluctuation areas tended to be distributed in areas with slight and significant increases (Fig. 3a, b). Low-fluctuation, relatively low-fluctuation, and moderate-fluctuation areas generally occurred in stable or significantly decreasing areas. Overall, 35.06% of the study area exhibited moderate fluctuation, which was mainly distributed in medium-low-, medium-, and medium-high-coverage zones (Fig. 4). Moderate fluctuations mostly occurred along riverbanks in the north-central part of the study area. Overall, 27.50% of the study area exhibited relatively low fluctuation, which was mainly distributed in the west, northernmost, and central-east parts. Low fluctuation mostly occurred in medium-high-coverage and medium-coverage zones. Overall, 19.78% of the study area had relatively high fluctuation, which was mainly distributed in the medium-coverage and medium-low-coverage zones. Overall, 16.38% of the study area exhibited high fluctuation, which was mainly distributed in medium-low- and low-coverage zones in the northeastern and southernmost parts of the study area.

**Table 3** Percentage area with different trends in FVC

Type of change	Percentage area (%)
Significant decrease	18.25
Slight decrease	5.20
Insignificant change	51.99
Slight increase	5.35
Significant increase	19.21

Detection of influencing factors

Parameter optimization

In the aspect of spatial scale effect, *q* values of nearly all factors tended to increase with increasing grid

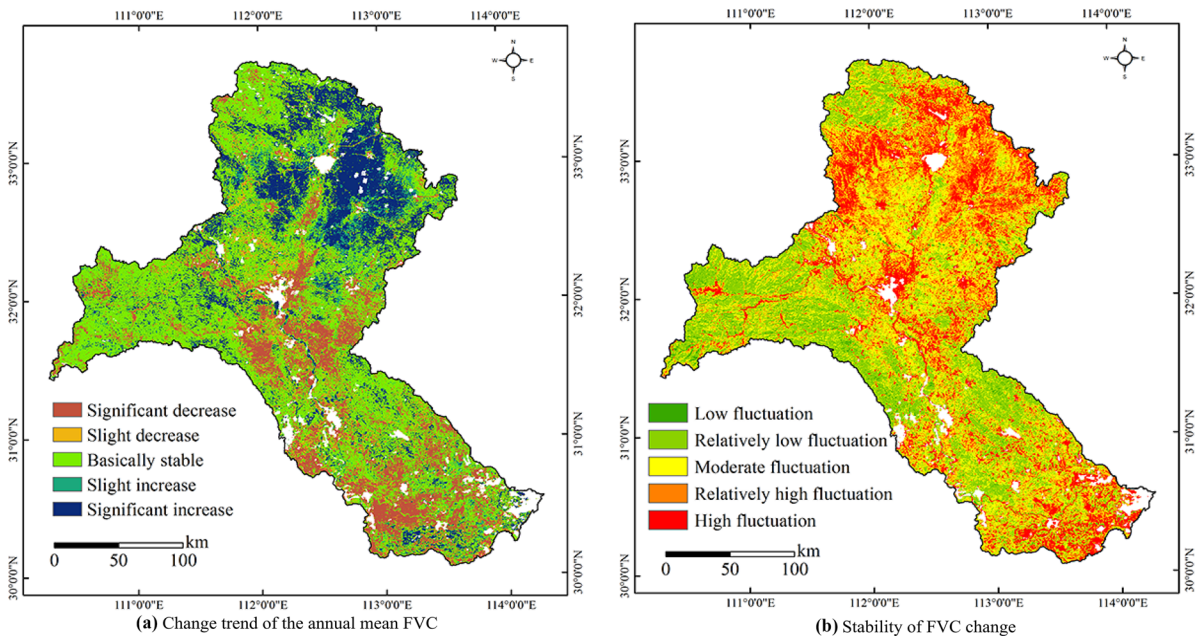


**Fig. 3** a, b Change characteristics of annual mean FVC in MLHB from 2001 to 2018

size, but with high fluctuation. In contrast,  $q$  values were relatively moderate and stable at a 5 km×5 km scale (Fig. 5a). Ranks of most factors, especially factors with higher influence, remained relatively stable at the 5 km×5 km grid size (Fig. 5b). Moreover, this

scale provided meaningful information on geographic variation in FVC at the ecological scale. Thus, 5 km was chosen as the optimal grid size for geographical detector analysis in this study.

**Fig. 4** Area statistics of changes to stability in FVC for different variation types in MLHB during 2001–2018

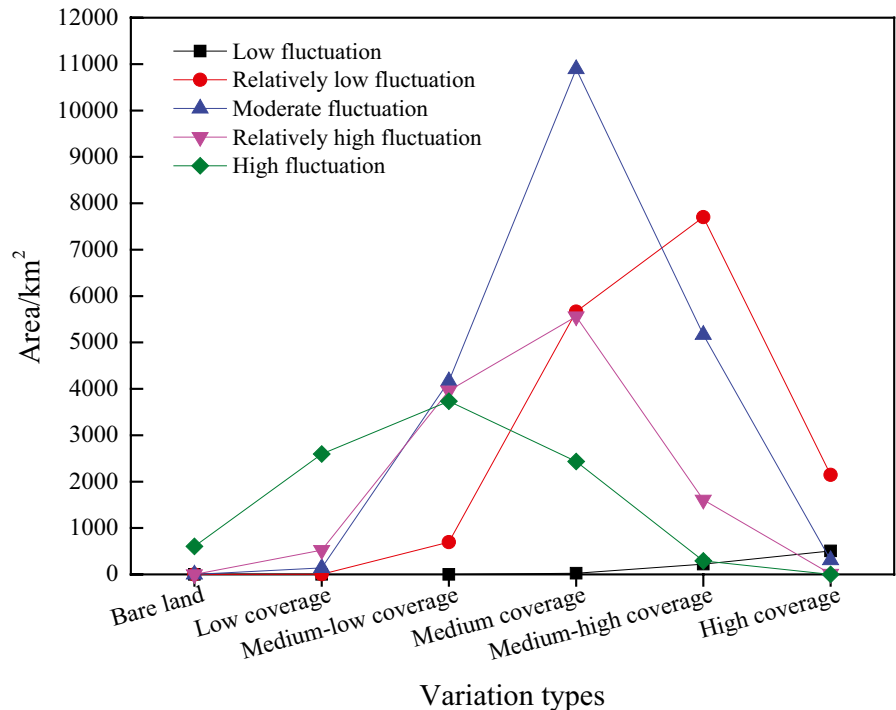




**Table 4** Percentage area with different trends in FVC

CV <sub>FVC</sub>	Degree in fluctuation	Percentage area (%)
CV <sub>FVC</sub> < 0.05	Low fluctuation	1.27
0.05 ≤ CV <sub>FVC</sub> < 0.10	Relatively low fluctuation	27.50
0.10 ≤ CV <sub>FVC</sub> < 0.15	Moderate fluctuation	35.06
0.15 ≤ CV <sub>FVC</sub> < 0.20	Relatively high fluctuation	19.78
CV <sub>FVC</sub> ≥ 0.20	High fluctuation	16.38

For the spatial data discretization effect, *q* values varied with classification method used (Table 3 in the Appendix), while no specific relationships were found between *q* values and zoning methods. For instance, the natural break and quantile methods produced relatively consistent results for both natural and human factors. Based on the characteristics of factors and spatial data, the natural break (Jenks) method was used to classify precipitation (eight grades, represented as A1–A8), temperature (eight grades), and population density (five grades). Prior knowledge, range, and distribution characteristics of the data were considered when manually classifying the other factors. Detailed classification information in 2018 is provided in Table 4 in the Appendix.

*Influence of natural and human factors*

All 10 factors had a significant impact on changes to FVCs (*p* < 0.05) over three time periods (2001, 2009, and 2018). In 2018, *q* values of various natural and anthropogenic factors were ranked as follows: slope > landform type > distance to water >

NTL > elevation > vegetation type > precipitation > Pd > temperature > soil type (Fig. 6). For the 10 categories of natural and human factors, *q* values of slope and landform type accounted for more than 20% of change to FVC, respectively. *q* values of all other factors were between 10 and 20%. Therefore, both natural and anthropogenic factors strongly influenced changes to FVC since 2001 in the study area. In 2001, the largest influencing factor was precipitation, explaining 42.64% of change to FVC (Fig. 6), followed by temperature (16.22%), elevation (15.13%), and slope (15.13%). In 2009, the largest influencing factor was slope (24.59%), followed by landform type (17.90%), precipitation (15.29%), and elevation (13.01%). In 2018, slope had the largest influence (32.05%), followed by landform type (24.09%), distance to water (16.71%), and NTL (15.48%). Therefore, precipitation was the primary factor affecting spatial differentiation in FVC in 2001, whereas it was slope in 2009 and 2018. Influence of climatic factors declined, whereas that of topography increased to become the dominant factor. Influence of distance to water and NTL also gradually increased. Distance to water became the third largest influential factor in 2018, followed by NTL. Influence of human activity on change to vegetation coverage gradually increased.

*Interaction between factors*

Overall, the joint impact of any two influencing factors of change on FVC was greater than that of each single factor. The interaction between detected factors on FVC was bi-enhanced or nonlinear-enhanced.

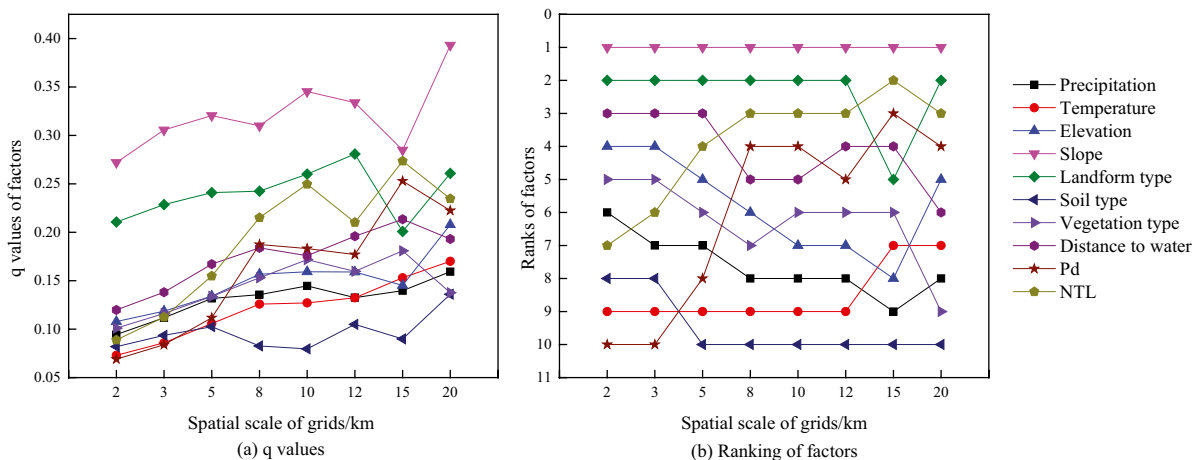
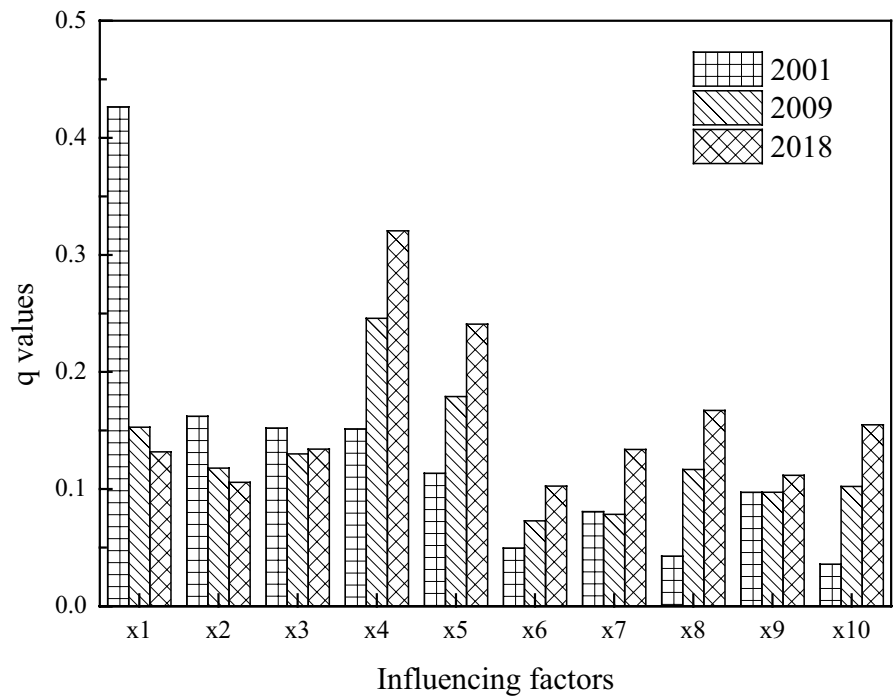


**Fig. 5** a, b Scale effects on results of the geographical detector

**Fig. 6** Changes to the  $q$  value of the 10 factors in 2001, 2009, and 2018



The synergic effect of human and other factors on FVC, for example, in 2018, was as follows:  $x_{10} \cap x_4$  (0.416) >  $x_{10} \cap x_5$  (0.358) >  $x_{10} \cap x_8$  (0.300) >  $x_{10} \cap x_1$  (0.277) >  $x_{10} \cap x_3$  (0.266) >  $x_{10} \cap x_6$  (0.260) >  $x_{10} \cap x_7$  (0.255) >  $x_{10} \cap x_2$  (0.237) >  $x_{10} \cap x_9$  (0.184) (Table 5 in the Appendix). The interaction between NTL and soil type presented a nonlinear enhancement effect. However, the relationship between NTL and all other factors presented a mutual enhancement effect. The following interactions occurred between topography and other factors on FVC, for example:  $x_1 \cap x_4$  (0.456) >  $x_4 \cap x_{10}$  (0.416) >  $x_4 \cap x_9$  (0.401) >  $x_2 \cap x_4$  (0.384) >  $x_4 \cap x_8$  (0.380) >  $x_4 \cap x_6$  (0.378) >  $x_4 \cap x_7$  (0.364) >  $x_3 \cap x_4$  (0.357) >  $x_4 \cap x_5$  (0.339) (Table 5 in the Appendix). The interaction between slope and precipitation presented a nonlinear enhancement effect. In contrast, the interaction between slope and all other factors presented mutual enhancement effects.

The interaction of precipitation and slope was consistently highest in 2001, 2009, and 2018 (Table 6 in the Appendix). In 2001, the interaction of precipitation and elevation was the second highest, followed by the interaction of precipitation and temperature. In 2009 and 2018, the interaction of slope and NTL was the second highest, followed by the interaction of slope and population density. The interaction between precipitation and topography was more significant

than any other two factors, or any single factor since 2001. Interactions occurred between human and topographical factors for FVC and had a gradually increasing significance on FVC change over the research period.

*Suitable range/type of factors for vegetation coverage*

The optimal range or type of factors for vegetation growth was explored with the risk detector module. Factors that had a relatively high influence and greatest changes are discussed here.

**Adaptation range of precipitation to FVC**

FVC did not always increase with increasing precipitation; specifically, as precipitation increased, vegetation coverage first increased and then decreased. Maximum mean FVC was greatest in A5 during 2018 (Fig. 7a). Overall, vegetation coverage was largest at a precipitation range of 1003.5–1078.4 mm. Precipitation has a distinct suitable range for vegetation, and moderate precipitation would promote an increase of vegetation coverage in the study area.

**Adaptation range of slope to FVC**

Vegetation coverage fluctuated with increasing slope (Fig. 7b). Mean

FVC was largest for a slope range of 5–15° in the three periods. Within this range, this topographic factor was conducive to vegetation growth. Maximum mean FVC in the area was 0.62 in 2018. Mean FVC for slopes > 15° (slope of 15–35° and 35–55° accounted for 7.83% and 0.16% of the study area, respectively) in 2018 was 0.58 and was second to areas with slopes between 5 and 15°. There was little human interference in these slope areas, resulting in high vegetation coverage. FVC was intermediate for all slope areas in low terrain slope (0–0.5°), such as valley plains. For slopes of 0.5–5°, where most human activity occurs, vegetation coverage was relatively low, particularly for 0.5–2° slopes.

**Adaptation of landform type to FVC** Mean FVC fluctuated with landform type (Fig. 7c). Mean FVC of small, medium, and large undulating mountains exceeded 0.55, with these landform types benefiting vegetation growth. Small undulating mountains had the highest FVC (exceeding 0.60 in 2018). Platforms and hills had mean FVCs of less than 0.50. The lowest FVC of 0.45 was recorded for platforms in 2018.

**Adaptation range of distance to the water on FVC** As distance from water body increased, vegetation coverage also increased (Fig. 7d). Mean FVC in regions 0–1 km and 30–60 km from water bodies differed to other regions. At 30–60 km from water bodies, mean FVC peaked at 0.65 in 2018, showing that these areas are more suitable for vegetation growth than other areas. At 0–1 km from water bodies, vegetation coverage was lowest in 2018 (0.44), with poor conditions for vegetation growth. In fact, compared to all other distances to water bodies, this area had the largest decrease in vegetation coverage since 2001. At 1–3 km from water bodies, vegetation coverage showed a continuous downward trend, indicating degraded vegetation growth. The second highest mean FVC was obtained at 20–30 km from water bodies, first increasing and then decreasing over the study period. Except for distances of 0–1 km, 1–3 km, and 20–30 km from water bodies, vegetation coverage of all other areas increased since 2001, particularly at 3–20 km distance. In 2001, FVC at 3–20 km distance from water bodies was lower than that at 0–3 km distance. In contrast, in 2018, FVC at 3–20 km distance was much higher than that at 0–3 km distance, showing that vegetation

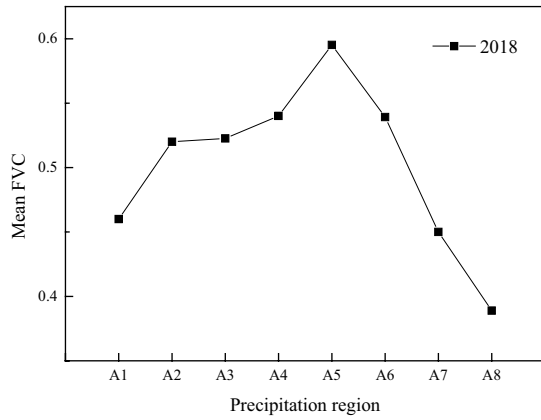
coverage improved at 3–20 km distances from water bodies.

**Adaptation range of NTL to FVC** Vegetation coverage generally decreased with increasing nighttime light. Mean FVC was highest for B1 (0.53) (Fig. 7e) than for all other regions during 2001 and 2018 and was considered more suitable for vegetation growth than other regions. Vegetation coverage was optimal at 0–0.1 w/m<sup>2</sup>, where human activity was low. More economically developed areas with brighter nighttime lights had lower vegetation coverage. For instance, NTL was highest in B7, where FVC was lowest out of the seven regions, which primarily contained built-up urban areas. Thus, changes to FVC were largely affected by human activity.

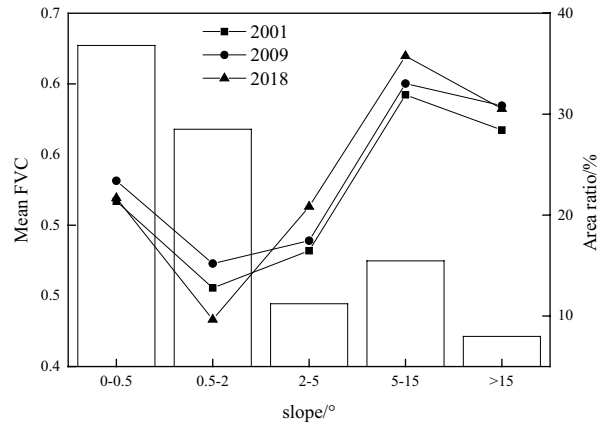
## Discussion

Improving detection of factors driving vegetation coverage

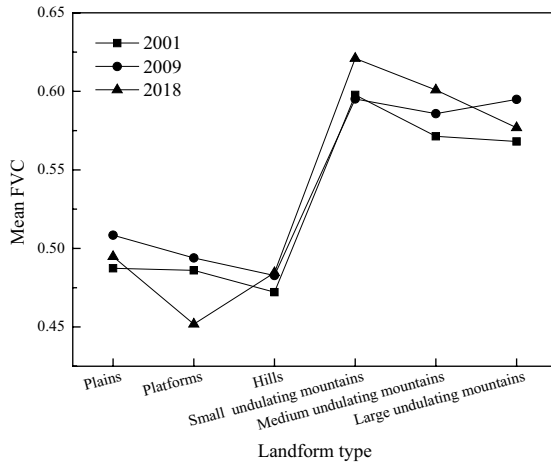
This study provided a first step towards understanding the factors driving changes to vegetation coverage in a small watershed of a humid valley plain, where major changes to the ecological environment, social economy, and their interactions have occurred since 2001. Quantitatively determining contribution of factors driving change to vegetation at multiple time periods is essential for implementing appropriate management of vegetation ecosystems. Unlike using traditional statistical methods (Fotheringham et al., 2000; Getis & Ord, 2010; Matheron, 1963), this study used the geographical detector model to identify and differentiate the relative important driving forces and their interaction to FVC change based on spatial variation information and avoiding complex parameter settings. Input data used in the geographical detector model is essentially raster format (Wang & Xu, 2017). Thus, it is essential to calculate how the actual area size represented by the grid affects the results of the geographical detector (Gao et al., 2021; Ju et al., 2016; Song et al., 2020). In contrast to previous studies with little consideration to the representation of different grid cell sizes when using the geographical detector, the current study considered the scale effect, selecting a reasonable analysis size by comparing the  $q$  values of different spatial units.



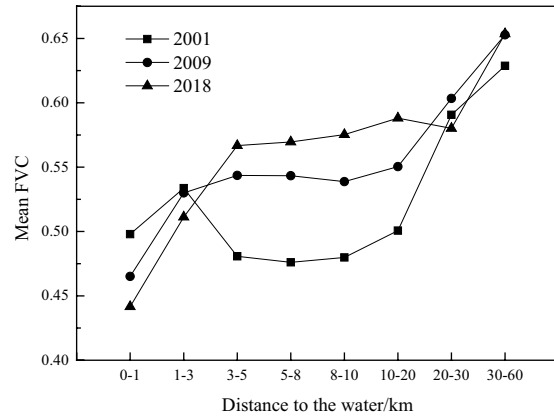
(a) Mean annual FVC of sub-regions in relation to precipitation



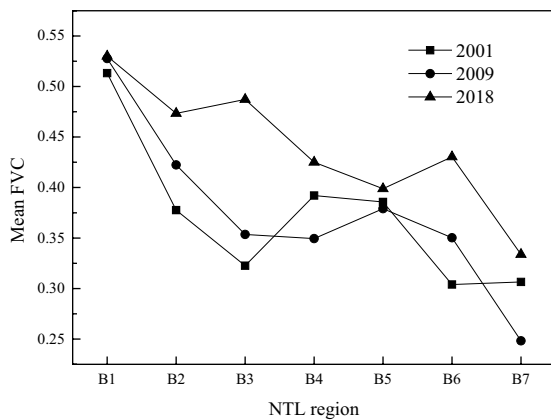
(b) Mean FVC for different slopes



(c) Mean FVC of different landform types



(d) Mean FVC in different water buffer zones



(e) Mean FVC of sub-regions with respect to NTL

Fig. 7 a–e Mean FVC of subregions or subcategories in relation to selected factors in 2001, 2009, and 2018

## Change to vegetation cover influenced by natural factors

### *Climatic factors*

Climatic factors are generally considered to be important biophysical components affecting vegetation growth and development (Jiang et al., 2021; Wang et al., 2021). Vegetation type and quantity are closely associated with precipitation and temperature (Jiao et al., 2021). Previous studies showed that vegetation cover is significantly correlated with precipitation and temperature in Mainland China, including the Yangtze River Basin (Chen et al., 2020; Jiao et al., 2021). The current study showed that FVC in MLHB was altered by precipitation and temperature; however, the degree to which these two climate factors affected FVC has gradually declined since 2001, especially precipitation. However,  $q$  values of interaction between precipitation and other factors (including temperature, elevation, slope, landform type, and soil type) exceeded the arithmetic sum of their respective  $q$  values. Thus, precipitation noticeably impacted FVC, with this influence being primarily reflected in its interaction with other natural factors. For instance, the interaction between precipitation and slope consistently had the largest  $q$  value, whereas the  $q$  value of precipitation in 2009 and 2018 was ranked third or lower out of all 10 factors.

### *Slope*

Slope had a gradually increasing significant influence on FVC in the study area since 2001. It is related to ecological restoration measures in some slope areas; however, it is also related to land use and land cover change in different slope areas. Notably, in the implementation of ecological restoration measures, the factor slope had become an important deciding condition for determining the area where land use type could change (Zhang et al., 2020a). The Hanjiang River Basin is an important ecological conservation area of the Yangtze River Basin (Yu, 2018). Optimal allocation of vegetation is required to implement ecological recovery projects. According to water conservation functions in the Hanjiang River Basin during 2010,

forests, shrubs, grasslands, unused land, and farmland slopes ( $> 25^\circ$ ) were included in the scope of ecological restoration (Yu, 2018). For slopes of  $0.5\text{--}2^\circ$ , FVC has declined since 2001, but noticeably increased for slopes  $2\text{--}5^\circ$  over the same period (Fig. 7b). This phenomenon was related to land use and land cover change in the areas with different slopes affected by the policy of returning farmland to lakes, expansion of built-up urban areas, and improvement of the urban living environment (Li et al., 2020; Liu et al., 2020). Analysis of land use change in the study area from 2000 to 2015 (Table 7 in the Appendix) showed that the total area of residential and other construction land increased by  $934\text{ km}^2$  and the total water area increased by  $518\text{ km}^2$ , whereas the total area of cultivated land decreased by  $1399\text{ km}^2$ . The net transfer of cultivated land to water areas, residential land, and forested land was  $480\text{ km}^2$ ,  $789\text{ km}^2$ , and  $42\text{ km}^2$ , respectively. Studies have shown that active areas of land use change were mainly distributed on both sides of the river, the plain, hinterland, and hilly areas (Yang, 2017). Changes to vegetation coverage in areas with different slopes reflect the impact of human activity on the natural environment, to some extent.

### *Distance to water*

In the study area, vegetation grew better with increasing distance from water bodies. Large areas of floodplains and desertified land were located in the 1-km buffer zone from water bodies, which were not conducive to growth of vegetation (Chen et al., 2013; Wang et al., 2019b); consequently, vegetation coverage was relatively low. At the 0–3 km buffer from waterbodies, FVC declined during 2001 and 2018. Construction of hydraulic facilities, such as levees and revetments (Zhang et al., 2020b), on either side of the river weakens the direct recharging of river water to groundwater (Huang et al., 2021), to a certain extent, reducing vegetation coverage in areas close to the river. Furthermore, areas with vegetation cover degradation were mainly concentrated along the river during 2018 and 2001, which could be seen from the map showing the difference of FVC between July 2018 and July 2001 (Fig. 1 in the Appendix).

## Influence of human factors

The influence of Pd and NTL increased over the study period, and their interaction with other natural factors was enhanced; thus, the influence of human activity increased over time. Human activity can either promote the increase of vegetation coverage or reduce it. Urban expansion and urbanization of populations might reduce vegetation coverage around cities. When urbanization reaches a certain stage, peoples' requirements for green space increase, and vegetation coverage of urban areas might also increase (Pu, 2016; Teng, 2011). This phenomenon is shown with respect to FVC changes in the B7 region (Fig. 7e), the highest NTL zone. In B7, FVC first declined and then increased, which might be attributed to urbanization of populations and increased public awareness on environmental protection and ecological conservation (Cheng et al., 2021). Statistics on urbanization rate of populations in two major cities, Xiangyang and Jingmen, located in the middle and lower reaches of Hanjiang River Basin, confirmed rapid urbanization from 2001 to 2018 (Table 8 in the Appendix) (Hubei Provincial Bureau of Statistics, 2001–2018). With the influx of population to urban areas, built-up land expanded and vegetated areas declined. With subsequent improvement in living standards and better awareness of the ecological environment, people paid more and more attention to the living environment, and urban green space increased sharply, especially in Xiangyang City (Table 8 in the Appendix) (Hubei Provincial Bureau of Statistics, 2001–2018); an increase in the area of green land during 2009 and 2018 was double than that during 2001 and 2009, with vegetation coverage increasing.

Afforestation and other ecological restoration measures are important artificial measures conducive to increasing vegetation coverage, especially in degraded land areas (Fig. 2a, b in the Appendix). For instance, the afforested area of Xiangyang City exceeded 10,000 ha annually from 2001 to 2017 (Fig. 3 in the Appendix) (National Forestry Administration, 2001–2018), reaching 30,000 ha in 2003. Furthermore, the afforested area in Jingmen City has mostly exceeded 5000 ha per year and exceeded 15,000 ha in 2003. Increased interactions between human activity and terrain also demonstrated improved transformation of nature. Selection of spaces for ecological restoration of vegetation

requires regulations on how these spaces are distributed and which tree species are planted. Particularly, more artificial forests than natural forests were present in the study area (Xiao et al., 2015). Thus, better vegetation protection, restoration measures, and land resources management are needed.

## Limitations and uncertainties

Compared to traditional approaches of linear regression and correlation analysis for analyzing changes to vegetation cover, the geographic detector model effectively detects spatial changes, analyzes factors driving these phenomena, and identifies multi-factor interactions. However, the geographic detector model is ultimately a statistical model that reveals causal laws and cannot be used to explain causal mechanisms. Therefore, determining reasons for the results requires further background investigation and additional analyses. In addition, future studies should incorporate more factors contributing to FVC. Certain studies have shown that soil moisture is an important factor limiting vegetation growth, especially in areas subject to soil erosion and land degradation (D'Odorico et al., 2007; Rodriguez-Iturbe et al., 1999). Thus, soil moisture should be considered in future studies. Moreover, land use also largely determines changes to vegetation cover at regional scales. However, here, land use was included as a parameter to calculate FVC and was not considered as a human factor. Furthermore, the study area contained more pure forests than mixed forests. These pure forest ecosystems had simple plant community composition, resulting in their being highly fragile with poor resistance to pests. Therefore, the influence of insect pests should also be included as a factor influencing change to FVC in future studies.

## Conclusions

This study explored spatiotemporal variation patterns of vegetation coverage and quantified how natural and anthropogenic factors altered vegetation coverage between 2001 and 2018 in MLHB using the geographical detector to map change based on MODIS EVI data.

The study area was dominated by medium, medium-high, and medium-low vegetation coverage. Spatial distribution characteristics of FVC in the study area

were relatively high in south-central and the west and relatively low in the north and along the banks of the northernmost and southernmost sections of the middle and lower reaches of Hanjiang River Basin. The FVC of approximately half of the study area was relatively stable, while it declined and increased in about 23.45% and 24.56% of the total study area, respectively. The area with declining FVC was mainly distributed along the banks of Hanjiang River and its tributaries in the central and southern parts. The area with increasing FVC was mainly distributed on the northern plain. Overall, areas with higher FVC also had more stable FVC.

All the detected natural and anthropogenic factors had significant effects on changes to FVC in MLHB since 2001. The primary factors causing FVC to change were precipitation in 2001 and slope in 2018, followed by landform type, distance to water, and NTL in 2018. The degree of change of natural and human influence can be seen through the detection of influencing factors in multiple periods. Detected factors did not influence FVC independently, but interacted through reinforced or nonlinear enhancement. Interaction of precipitation and slope was consistently the largest from 2001 to 2018. The interaction between human and topographic factors impacted FVC with gradually increasing significance over the research period. These findings reminded that the impacts of various factors driving changes to FVC in MLHB should be comprehensively considered to implement appropriate management plans for protection, utilization, and restoration of vegetation. Importantly, terrain characteristics, water resource conditions, and human development should be considered to optimize these practices. Ranges of precipitation, slope, distance to water, and NTL suitable for vegetation growth were 968.6–1040.9 mm, 5–15°, 30–60 km, and 0–0.1 W/km<sup>2</sup>, respectively. Landform type with largest FVC was in small undulating mountains. This information can be used to delineate management approaches for habitat restoration in MLHB. The results of this study advance current understanding on factors regulating change to vegetation coverage in this humid valley plain of China. Our findings could be used as a scientific basis for the conservation and restoration of the ecological environment in the Hanjiang River Basin, China.

**Author contribution** Conceptualization, Y. Y.; methodology, Y. Y. and X. B.; software, H. L., W. Z., and X. B.; validation, Y. Y., S. W., and J. L.; investigation, Y. Y. and X. B.; resources, Y. Y. and H. L.; writing—original draft preparation, Y. Y.; writing—review and editing, X. B.; visualization, H. L.; supervision, X. B. and Y. C.; project administration, Y. Y. and X. B.; funding acquisition, Y. Y., X. B., and Y. C. All authors have read and agreed to the published version of the manuscript.

**Funding** This research was funded by the National Natural Science Foundation of China (grant numbers 41901235, 41704081, and 41877428) and the Fundamental Research Funds for the Central Universities, South-Central Minzu University (grant number CZY20033).

**Data availability** All the data used in this study are available from the corresponding author on reasonable request.

## Declarations

**Conflict of interest** The authors declare no competing interests.

## References

- Cao, R., Jiang, W. G., Yuan, L. H., Wang, W. J., Lv, Z. L., & Chen, Z. (2014). Inter-annual variations in vegetation and their response to climatic factors in the upper catchments of the Yellow River from 2000 to 2010. *Journal of Geographical Sciences*, 24(6), 963–979. <https://doi.org/10.1007/s11442-014-1131-1>
- Carlson, T. N., & Ripley, D. A. (1997). On the relation between NDVI, fractional vegetation cover, and leaf area index. *Remote Sensing of Environment*, 62(3), 241–252. [https://doi.org/10.1016/S0034-4257\(97\)00104-1](https://doi.org/10.1016/S0034-4257(97)00104-1)
- Chen, H., Du, Y., Xiao, F., Wang, X. L., Yan, Y., & Li, Y. Z. (2013). Relationship between temporal and spatial change of vegetation index and desertification land dynamic in the plain area of middle reaches of the Hanjiang River. *Resources and Environment in the Yangtze Basin*, 22(9), 1221–1226. (in Chinese).
- Chen, H., Guo, S., Xu, C. Y., & Singh, V. P. (2007). Historical temporal trends of hydro-climatic variables and runoff response to climate variability and their relevance in water resource management in the Hanjiang basin. *Journal of Hydrology*, 344(3–4), 171–184. <https://doi.org/10.1016/j.jhydrol.2007.06.034>
- Chen, T., Xia, J., Zou, L., & Hong, S. (2020). Quantifying the influences of natural factors and human activities on NDVI changes in the Hanjiang River Basin, China. *Remote Sensing*, 12(22), 3780. <https://doi.org/10.3390/rs12223780>
- Cheng, P., Min, M., Hu, W. Y., & Zhang, A. L. (2021). A framework for fairness evaluation and improvement of urban green space: A case of Wuhan metropolitan area in China. *Forests*, 12(7), 890. <https://doi.org/10.3390/f12070890>

- De Boer, T. A. (1983). Vegetation as an indicator of environmental changes. *Environmental Monitoring and Assessment*, 3, 375–380. <https://doi.org/10.1007/BF00396232>
- Deng, L. L., Yin, J. B., Tian, J., Li, Q. X., & Guo, S. L. (2021). Comprehensive evaluation of water resources carrying capacity in the Han River Basin. *Water*, 13(3), 249. <https://doi.org/10.3390/w13030249>
- Ding, Y. L., Zheng, X. M., Zhao, K., Xin, X. P., & Liu, H. J. (2016). Quantifying the impact of NDVI<sub>soil</sub> determination methods and NDVI<sub>soil</sub> variability on the estimation of fractional vegetation cover in Northeast China. *Remote Sensing*, 8(1), 29. <https://doi.org/10.3390/rs8010029>
- D'Odorico, P., Caylor, K., Okin, G. S., & Scanlon, T. M. (2007). On soil moisture–vegetation feedbacks and their possible effects on the dynamics of dryland ecosystems. *Journal of Geophysical Research-Biogeosciences*, 112(G4), 231–247. <https://doi.org/10.1029/2006JG000379>
- Feng, D. R., Yang, C., Fu, M. C., Wang, J. M., Zhang, M., Sun, Y. Y., & Bao, W. K. (2020). Do anthropogenic factors affect the improvement of vegetation cover in resource-based region? *Journal of Cleaner Production*, 271, 122705. <https://doi.org/10.1016/j.jclepro.2020.122705>
- Fernandes, R., & Leblanc, S. G. (2005). Parametric (modified least squares) and non-parametric (Theil-Sen) linear regressions for predicting biophysical parameters in the presence of measurement errors. *Remote Sensing of Environment*, 95(3), 303–316. <https://doi.org/10.1016/j.rse.2005.01.005>
- Fotheringham, A.S., Brunson, C., & Charlton, M.E. (2000). *Quantitative geography: Perspectives on spatial data analysis*. Sage.
- Gao, F., Li, S. Y., Tan, Z. Z., Wu, Z. F., Zhang, X. M., Huang, G. P., & Huang, Z. W. (2021). Understanding the modifiable areal unit problem in dockless bike sharing usage and exploring the interactive effects of built environment factors. *International Journal of Geographical Information Science*, 35(9), 1905–1925. <https://doi.org/10.1080/13658816.2020.1863410>
- Getis, A., & Ord, J. K. (2010). *The analysis of spatial association by use of distance statistics* (pp. 189–206). Springer.
- Gilbert, R. O. (1987). *Statistical methods for environmental pollution monitoring*. Van Nostrand Reinhold Company.
- Gutman, G., & Ignatov, A. (1998). The derivation of the green vegetation fraction from NOAA/AVHRR data for use in numerical weather prediction models. *International Journal of Remote Sensing*, 19(8), 1533–1543. <https://doi.org/10.1080/014311698215333>
- Han, J. J., Wang, J. P., Chen, L., Xiang, J. Y., Ling, Z. Y., Li, Q. K., & Wang, E. L. (2021). Driving factors of desertification in Qaidam Basin, China: An 18-year analysis using the geographic detector model. *Ecological Indicators*, 124, 107404. <https://doi.org/10.1016/j.ecolind.2021.107404>
- He, W. M., He, Q. L., & Zhou, J. (2015). Soil weathering-water environment-ecological risks in Hanjiang River Basin, China. *Quaternary International*, 380, 297–304. <https://doi.org/10.1016/j.quaint.2015.01.017>
- Holben, B. N. (1986). Characteristics of maximum-value composite images from temporal AVHRR data. *International Journal of Remote Sensing*, 7, 1417–1434. <https://doi.org/10.1080/01431168608948945>
- Hong, X. J., Guo, S. L., Wang, L., Yang, G., Liu, D. D., Guo, H. J., & Wang, J. (2016). Evaluating water supply risk in the middle and lower reaches of Hanjiang River Basin based on an integrated optimal water resources allocation model. *Water*, 8(9), 364. <https://doi.org/10.3390/w8090364>
- Huang, Y. Y., Xie, T., Fei, D. W., & Yan, J. (2021). Working behaviour feedback of composite geomembranes based on seepage monitoring data. *Geosynthetics International*, 28(6), 609–623. <https://doi.org/10.1680/jgein.21.00025>
- Hubei Provincial Bureau of Statistics. (2001–2018). *Hubei statistical yearbook*. China Statistics Press.
- Iizuka, K., Kato, T., Silsigia, S., Soufiningrum, A. Y., & Kozan, O. (2019). Estimating and examining the sensitivity of different vegetation indices to fractions of vegetation cover at different scaling grids for early stage acacia plantation forests using a fixed-wing UAS. *Remote Sensing*, 11(15), 1816. <https://doi.org/10.3390/rs11151816>
- Jiang, M. C., He, Y. X., Song, C. H., Pan, Y. P., Qiu, T., & Tian, S. F. (2021). Disaggregating climatic and anthropogenic influences on vegetation changes in Beijing-Tianjin-Hebei region of China. *Science of the Total Environment*, 786, 147574. <https://doi.org/10.1016/j.scitotenv.2021.147574>
- Jiao, K. W., Gao, J. B., Liu, Z. H., Wu, S. H., & Fletcher, T. L. (2021). Revealing climatic impacts on the temporal and spatial variation in vegetation activity across China: Sensitivity and contribution. *Advances in Climate Change Research*, 12(3), 409–420. <https://doi.org/10.1016/j.accre.2021.04.006>
- Jin, H. Y., Chen, X. H., Zhong, R. D., Wu, P., & Li, D. (2021). Spatio-temporal changes of precipitation in the Hanjiang River Basin under climate change. *Theoretical and Applied Climatology*, 146(3–4), 1441–1458. <https://doi.org/10.1007/s00704-021-03801-y>
- Ju, H. R., Zhang, Z. X., Zuo, L. J., Wang, J. F., Zhang, S. R., Wang, X., & Zhao, X. L. (2016). Driving forces and their interactions of built-up land expansion based on the geographical detector - A case study of Beijing, China. *International Journal of Geographical Information Science*, 30(11), 2188–2207. <https://doi.org/10.1080/13658816.2016.1165228>
- Kendall, M. G. (1948). *Rank correlation methods*. Griffin.
- Kong, D. X., Miao, C. Y., Borthwick, A. G. L., Lei, X. H., & Li, H. (2018). Spatiotemporal variations in vegetation cover on the Loess Plateau, China, between 1982 and 2013: Possible causes and potential impacts. *Environmental Science and Pollution Research*, 25(14), 13633–13644. <https://doi.org/10.1007/s11356-018-1480-x>
- Li, J. J., Peng, S. Z., & Li, Z. (2017). Detecting and attributing vegetation changes on China's Loess Plateau. *Agricultural and Forest Meteorology*, 247, 260–270. <https://doi.org/10.1016/j.agrformet.2017.08.005>
- Li, M. M., Wu, B. F., Yan, C. Z., & Zhou, W. F. (2004). Estimation of vegetation fraction in the upper basin of Miyun reservoir by remote sensing. *Resource Science*, 26, 153–159. (in Chinese).
- Li, S. S., Zhang, L., Du, Y., Zhuang, Y. H., & Yan, C. C. (2020). Anthropogenic impacts on streamflow-compensated climate change effect in the Hanjiang River Basin, China. *Journal of Hydrologic Engineering*, 25(1), 04019058. [https://doi.org/10.1061/\(asce\)/jhe.1943-5584.0001876](https://doi.org/10.1061/(asce)/jhe.1943-5584.0001876)
- Li, Y., Zheng, Z. C., Qin, Y. C., & Rong, P. J. (2021). Relative contributions of natural and man-made factors to



- vegetation cover change of environmentally sensitive and vulnerable areas of China. *Journal of Cleaner Production*, 321, 128917. <https://doi.org/10.1016/j.jclepro.2021.128917>
- Liu, H., Huang, Y., & Zheng, L. (2020). Effects of climate and human activities on vegetation cover changes in Danjiangkou water source areas. *Transactions of the Chinese Society of Agricultural Engineering*, 36, 97–105. (in Chinese).
- Liu, Y. X., Liu, S. L., Sun, Y. X., Li, M. Q., An, Y., & Shi, F. N. (2021). Spatial differentiation of the NPP and NDVI and its influencing factors vary with grassland type on the Qinghai-Tibet Plateau. *Environmental Monitoring and Assessment*, 193(1), 1–21. <https://doi.org/10.1007/s10661-020-08824-y>
- Mann, H. B. (1945). Nonparametric test against trend. *Econometrica*, 13, 245–259. <https://doi.org/10.2307/1907187>
- Matheron, G. (1963). Principles of geostatistics. *Economic Geology*, 58, 1246–1266. <https://doi.org/10.2113/gsecongeo.58.8.1246>
- Mu, X. H., Song, W. J., Gao, Z., McVicar, T. R., Donohue, R. J., & Yan, G. J. (2018). Fractional vegetation cover estimation by using multi-angle vegetation index. *Remote Sensing of Environment*, 216, 44–56. <https://doi.org/10.1016/j.rse.2018.06.022>
- National Forestry Administration. (2001–2018). *China forestry statistical yearbook*. China Forestry Publishing House.
- Nie, T., Dong, G. T., Jiang, X. H., & Lei, Y. X. (2021). Spatio-temporal changes and driving forces of vegetation coverage on the Loess Plateau of Northern Shaanxi. *Remote Sensing*, 13(4), 613. <https://doi.org/10.3390/rs13040613>
- Peng, W. F., Kuang, T. T., & Tao, S. (2019). Quantifying influences of natural factors on vegetation NDVI changes based on geographical detector in Sichuan, Western China. *Journal of Cleaner Production*, 233, 353–367. <https://doi.org/10.1016/j.jclepro.2019.05.355>
- Piao, S. L., Fang, J. Y., Zhou, L. M., Guo, Q. H., Henderson, M., Ji, W., Li, Y., & Tao, S. (2003). Interannual variations of monthly and seasonal normalized difference vegetation index (NDVI) in China from 1982 to 1999. *Journal of Geophysical Research-Atmospheres*, 108(D14), 4401. <https://doi.org/10.1029/2002JD002848>
- Pu, Y. P. (2016). *Study on impact assessment of land use change and coordinated development of society and economy under watershed scale*. Wuhan: Central China Normal University. Dissertation.
- Purevdorj, T., Tateishi, R., Ishiyama, T., & Honda, Y. (1998). Relationships between percent vegetation cover and vegetation indices. *International Journal of Remote Sensing*, 19, 3519–3535. <https://doi.org/10.1080/014311698213795>
- Qu, S., Wang, L. C., Lin, A. W., Yu, D. Q., Yuan, M. X., & Li, C. A. (2020). Distinguishing the impacts of climate change and anthropogenic factors on vegetation dynamics in the Yangtze River Basin, China. *Ecological Indicators*, 108, 105724. <https://doi.org/10.1016/j.ecolind.2019.105724>
- Rao, C. J. (2012). Analysis and suggestions on free allocation with preferential policy for initial emission permits. *Advanced Building Materials and Structural Engineering*, 461, 624–628. <https://doi.org/10.4028/www.scientific.net/AMR.461.624>
- Rodriguez-Iturbe, I., D’Odorico, P., Porporato, A., & Ridolfi, L. (1999). On the spatial and temporal links between vegetation, climate, and soil moisture. *Water Resource Research*, 35, 3709–3722. <https://doi.org/10.1029/1999WR900255>
- Sen, K. P. (1968). Estimates of the regression coefficient based on Kendall’s tau. *Journal of the American Statistical Association*, 63, 1379–1389. <https://doi.org/10.1080/01621459.1968.10480934>
- Shoshany, M., Kutiel, P., & Lavee, H. (1996). Monitoring temporal vegetation cover changes in Mediterranean and arid ecosystems using a remote sensing technique: Case study of the Judean Mountain and the Judean Desert. *Journal of Arid Environments*, 33, 9–21.
- Song, Y. Z., Wang, J. F., Ge, Y., & Xu, C. D. (2020). An optimal parameters-based geographical detector model enhances geographic characteristics of explanatory variables for spatial heterogeneity analysis: Cases with different types of spatial data. *GIScience & Remote Sensing*, 57(5), 593–610. <https://doi.org/10.1080/15481603.2020.1760434>
- Sun, C. F., Liu, Y., Song, H. M., Li, Q., Cai, Q. F., Wang, L., Fang, C. X., & Liu, R. S. (2020). Tree-ring evidence of the impacts of climate change and agricultural cultivation on vegetation coverage in the upper reaches of the Weihe River, Northwest China. *Science of the Total Environment*, 707, 136160. <https://doi.org/10.1016/j.scitotenv.2019.136160>
- Sun, W. Y., Song, X. Y., Mu, X. M., Gao, P., Wang, F., & Zhao, G. J. (2015). Spatiotemporal vegetation cover variations associated with climate change and ecological restoration in the Loess Plateau. *Agricultural and Forest Meteorology*, 209, 87–99. <https://doi.org/10.1016/j.agrformet.2015.05.002>
- Tang, W. X., Liu, S. G., Kang, P., Peng, X., Li, Y. Y., Guo, R., Jia, J. N., Liu, M. C., & Zhu, L. J. (2021). Quantifying the lagged effects of climate factors on vegetation growth in 32 major cities of China. *Ecological Indicators*, 132, 108290. <https://doi.org/10.1016/j.ecolind.2021.108290>
- Teng, M. J. (2011). *Planning ecological security patterns in a rapidly urbanizing context: A case study in Wuhan, China*. Wuhan: Huazhong Agricultural University. Dissertation.
- Tian, J., Liu, D. D., Guo, S. L., Pan, Z. K., & Hong, X. J. (2019). Impacts of inter-basin water transfer projects on optimal water resources allocation in the Hanjiang River Basin, China. *Sustainability*, 11(7), 2044. <https://doi.org/10.3390/su11072044>
- Verbesselt, J., Zeileis, A., & Herold, M. (2012). Near real-time disturbance detection using satellite image time series. *Remote Sensing of Environment*, 123, 98–108. <https://doi.org/10.1016/j.rse.2012.02.022>
- Volpe, V., Silvestri, S., & Marani, M. (2011). Remote sensing retrieval of suspended sediment concentration in shallow waters. *Remote Sensing of Environment*, 115(1), 44–54. <https://doi.org/10.1016/j.rse.2010.07.013>
- Walther, G. R., Post, E., Convey, P., Menzel, A., Parmesan, C., Beebee, T., Fromentin, J. M., & Hoegh-Guldberg, & O., Bairlein, F. (2002). Ecological responses to recent climate change. *Nature*, 416, 389–395. <https://doi.org/10.1038/416389a>
- Wang, C. Y., Wang, J. N., Cui, X., Wei, Y. Q., Sun, J., Niyati, N., Du, W. T., & Chen, Q. T. (2021). Spatio-temporal change in vegetation patterns and its climatic drivers in

- the core region of Three Parallel Rivers in southeast Tibet. *Geographical Research*, 40, 3191–3207. (in Chinese).
- Wang, J., Wang, K. L., Zhang, M. Y., & Zhang, C. H. (2015). Impacts of climate change and human activities on vegetation cover in hilly Southern China. *Ecological Engineering*, 81, 451–461. <https://doi.org/10.1016/j.ecoleng.2015.04.022>
- Wang, J. F., & Hu, Y. (2012). Environmental health risk detection with GeogDetector. *Environmental Modelling & Software*, 33, 114–115. <https://doi.org/10.1016/j.envsoft.2012.01.015>
- Wang, J. F., & Xu, C. D. (2017). Geodetector: Principle and prospective. *Acta Geographica Sinica*, 72, 116–134. (in Chinese).
- Wang, J. F., Li, X. H., Christakos, G., Liao, Y. L., Zhang, T., Gu, X., & Zheng, X. Y. (2010). Geographical detectors-based health risk assessment and its application in the neural tube defects study of the Heshun region, China. *International Journal of Geographical Information Science*, 24(1), 107–127. <https://doi.org/10.1080/13658810802443457>
- Wang, J. F., Zhang, T. L., & Fu, B. J. (2016a). A measure of spatial stratified heterogeneity. *Ecological Indicators*, 67, 250–256. <https://doi.org/10.1016/j.ecolind.2016.02.052>
- Wang, P. T., Zhang, L. W., Li, Y. J., Jiao, L., Wang, H., Yan, J. P., Lv, Y. H., & Fu, B. J. (2018). Spatio-temporal variations of the flood mitigation service of ecosystem under different climate scenarios in the Upper Reaches of Hanjiang River Basin, China. *Journal of Geographical Sciences*, 28(10), 1385–1398. <https://doi.org/10.1007/s11442-018-1551-4>
- Wang, W. M., Li, C. H., Shu, J. W., & Chen, W. (2019a). Changes of vegetation in Southern China. *Science China-Earth Sciences*, 62(8), 1316–1328. <https://doi.org/10.1007/s11430-018-9364-9>
- Wang, X. X., Jia, K., Liang, S. L., & Zhang, Y. Z. (2016b). Fractional vegetation cover estimation method through dynamic Bayesian network combining radiative transfer model and crop growth model. *IEEE Transactions on Geoscience and Remote Sensing*, 54(12), 7442–7450. <https://doi.org/10.1109/tgrs.2016.2604007>
- Wang, Y. C., Xiao, F., Feng, Q., Zhou, Y. D., Chen, M. M., & Du, Y. (2019b). Spatio-temporal changes of the water-level fluctuation zone and inundation areas in middle and lower reaches of the Hanjiang River. *Resources and Environment in the Yangtze Basin*, 28, 2727–2734. (in Chinese).
- Wang, Y. G., Zhang, W. S., Zhao, Y. X., Peng, H., & Shi, Y. Y. (2016c). Modelling water quality and quantity with the influence of inter-basin water diversion projects and cascade reservoirs in the middle-lower Hanjiang River. *Journal of Hydrology*, 541, 1348–1362. <https://doi.org/10.1016/j.jhydrol.2016.08.039>
- Wu, D. H., Wu, H., Zhao, X., Zhou, T., Tang, B. J., Zhao, W. Q., & Jia, K. (2014). Evaluation of spatiotemporal variations of global fractional vegetation cover based on GIMMS NDVI data from 1982 to 2011. *Remote Sensing*, 6(5), 4217–4239. <https://doi.org/10.3390/rs6054217>
- Wu, R. H., Zhao, J. J., Zhang, H. Y., Guo, X. Y., Ying, H., Deng, G. R., & Li, H. (2019). Wildfires on the Mongolian Plateau: Identifying drivers and spatial distributions to predict wildfire probability. *Remote Sensing*, 11(20), 2361. <https://doi.org/10.3390/rs11202361>
- Xiao, C. W., Huang, Z. J., Jin, T. W., Tian, S. S., Ruan, H. E., & Li, X. Y. (2015). Construction of ecological protection forestry pests prevention and control system in the Middle and Lower Reaches of Hanjiang River. *Hubei Agricultural Sciences*, 54, 619–622 + 626. (in Chinese).
- Xu, C., Wang, J., Hou, Y., & Yin, Q. (2020a). *Geodetector: Software for measure and attribution of stratified heterogeneity (SH)*. [www.geodetector.cn](http://www.geodetector.cn)
- Xu, J. H. (2002). *Mathematical methods in contemporary geography*. Higher Education Press.
- Xu, L. L., Yu, G. M., Tu, Z. F., Zhang, Y. C., & Tsendbazar, N. E. (2020b). Monitoring vegetation change and their potential drivers in Yangtze River Basin of China from 1982 to 2015. *Environmental Monitoring and Assessment*, 192(10), 1–18. <https://doi.org/10.1007/s10661-020-08595-6>
- Xu, Q., Dong, Y. X., Wang, Y. Y., Yang, R., & Xu, C. D. (2018). Determinants and identification of the northern boundary of China's tropical zone. *Journal of Geographical Sciences*, 28(1), 31–45. <https://doi.org/10.1007/s11442-018-1457-1>
- Yan, K., Gao, S., Chi, H. J., Qi, J. B., Song, W. J., Tong, Y. Y., Mu, X. H., & Yan, G. J. (2022). Evaluation of the vegetation-index-based dimidiate pixel model for fractional vegetation cover estimation. *IEEE Transactions on Geoscience and Remote Sensing*, 60, 1–14. <https://doi.org/10.1109/tgrs.2020.3048493>
- Yang, B. H., Dou, M., Xia, R., Kuo, Y. M., Li, G. Q., & Shen, L. S. (2020). Effects of hydrological alteration on fish population structure and habitat in river system: A case study in the mid-downstream of the Hanjiang River in China. *Global Ecology and Conservation*, 23, e01090. <https://doi.org/10.1016/j.gecco.2020.e01090>
- Yang, G. J., Pu, R. L., Zhang, J. X., Zhao, C. J., Feng, H. K., & Wang, J. H. (2013). Remote sensing of seasonal variability of fractional vegetation cover and its object-based spatial pattern analysis over mountain areas. *ISPRS Journal of Photogrammetry and Remote Sensing*, 77, 79–93. <https://doi.org/10.1016/j.isprsjprs.2012.11.008>
- Yang, L., Shen, F. X., Zhang, L., Cai, Y. Y., Yi, F. X., & Zhou, C. H. (2021). Quantifying influences of natural and anthropogenic factors on vegetation changes using structural equation modeling: A case study in Jiangsu Province China. *Journal of Cleaner Production*, 280, 124330. <https://doi.org/10.1016/j.jclepro.2020.124330>
- Yang, Q. (2017). *The study of land use spatio-temporal transformation and ecological security in the Hanjiang River Basin of Hubei*. Wuhan: Wuhan University. Dissertation.
- Yu, Y. T. (2018). *Zoning for ecological remediation and optimal allocation of vegetation based on water conservation functions in Hanjiang River Basin*. Nanjing: Nanjing University of Information Science and Technology. Dissertation.
- Yun, G. L., He, Y. R., Jiang, Y. T., Dou, P. F., & Dai, S. Q. (2019). PM<sub>2.5</sub> spatiotemporal evolution and drivers in the Yangtze River Delta between 2005 and 2015. *Atmosphere*, 10(2), 55. <https://doi.org/10.3390/atmos10020055>
- Zhan, Y. J., Fan, J. M., Meng, T. T., Li, Z. W., Yan, Y., Huang, J. J., Chen, D., & Sui, L. T. (2021). Analysis on vegetation cover changes and the driving factors in the mid-lower reaches of Hanjiang River Basin between 2001 and 2015.

- Open Geosciences*, 13(1), 675–689. <https://doi.org/10.1515/geo-2020-0259>
- Zhang, D. J., Ge, W. Y., & Zhang, Y. (2020a). Evaluating the vegetation restoration sustainability of ecological projects: A case study of Wuqi County in China. *Journal of Cleaner Production*, 264, 121751. <https://doi.org/10.1016/j.jclepro.2020.121751>
- Zhang, M., Lin, H., Long, X. R., & Cai, Y. T. (2021). Analyzing the spatiotemporal pattern and driving factors of wetland vegetation changes using 2000–2019 time-series Landsat data. *Science of the Total Environment*, 780, 146615. <https://doi.org/10.1016/j.scitotenv.2021.146615>
- Zhang, R. R., Qi, J. Y., Leng, S., & Wang, Q. F. (2022). Long-term vegetation phenology changes and responses to pre-season temperature and precipitation in Northern China. *Remote Sensing*, 14(6), 1396. <https://doi.org/10.3390/rs14061396>
- Zhang, X. F., Liao, C. H., Li, J., & Sun, Q. (2013). Fractional vegetation cover estimation in arid and semi-arid environments using HJ-1 satellite hyperspectral data. *International Journal of Applied Earth Observation and Geoinformation*, 21, 506–512. <https://doi.org/10.1016/j.jag.2012.07.003>
- Zhang, Y. Y., Cai, X. B., Yang, C., Li, E. H., Song, X. X., & Ban, X. (2020b). Long-term (1986–2018) evolution of channel bars in response to combined effects of cascade reservoirs in the middle reaches of the Hanjiang River. *Water*, 12(1), 136. <https://doi.org/10.3390/w12010136>
- Zhao, L., Dai, A. G., & Dong, B. (2018). Changes in global vegetation activity and its driving factors during 1982–2013. *Agricultural and Forest Meteorology*, 249, 198–209. <https://doi.org/10.1016/j.agrformet.2017.11.013>
- Zhuan, M. J., Chen, J., Shen, M. X., Xu, C. Y., Chen, H., & Xiong, L. H. (2018). Timing of human-induced climate change emergence from internal climate variability for hydrological impact studies. *Hydrology Research*, 49(2), 421–437. <https://doi.org/10.2166/nh.2018.059>
- Zuazo, V. H. D., & Pleguezuelo, C. R. R. (2008). Soil-erosion and runoff prevention by plant covers. *A Review. Agronomy for Sustainable Development*, 28(1), 65–86. <https://doi.org/10.1051/agro:2007062>

**Publisher's Note** Springer Nature remains neutral with regard to jurisdictional claims in published maps and institutional affiliations.

Springer Nature or its licensor (e.g. a society or other partner) holds exclusive rights to this article under a publishing agreement with the author(s) or other rightsholder(s); author self-archiving of the accepted manuscript version of this article is solely governed by the terms of such publishing agreement and applicable law.